



## Borates or phosphates? That is the question

J. Contreras-García, F. Izquierdo-Ruiz, M. Marqués and F. J. Manjón

*Acta Cryst.* (2020). **A76**, 197–205



**IUCr Journals**

CRYSTALLOGRAPHY JOURNALS ONLINE

Copyright © International Union of Crystallography

Author(s) of this article may load this reprint on their own web site or institutional repository provided that this cover page is retained. Republication of this article or its storage in electronic databases other than as specified above is not permitted without prior permission in writing from the IUCr.

For further information see <https://journals.iucr.org/services/authorrights.html>

# Borates or phosphates? That is the question

J. Contreras-García,<sup>a\*</sup> F. Izquierdo-Ruiz,<sup>b</sup> M. Marqués<sup>c</sup> and F. J. Manjón<sup>d\*</sup>

<sup>a</sup>Laboratoire de Chimie Théorique, UPMC, Sorbonne Universités and CNRS, Paris 75005, France, <sup>b</sup>Departamento de Química Física y Analítica, MALTA-Consolider Team, Universidad de Oviedo, Oviedo E-33006, Spain, <sup>c</sup>Centre for Science at Extreme Conditions and School of Physics and Astronomy, The University of Edinburgh, Edinburgh EH9 3FD, UK, and <sup>d</sup>Instituto de Diseño para la Fabricación y Producción Automatizada, MALTA-Consolider Team, Universitat Politècnica de València, Valencia 46022, Spain. \*Correspondence e-mail: julia.contreras.garcia@gmail.com, fjmanjon@fis.upv.es

Received 11 September 2019

Accepted 16 December 2019

Edited by P. M. Dominiak, University of Warsaw, Poland

**Keywords:** borates; topology; electron density; nomenclature.

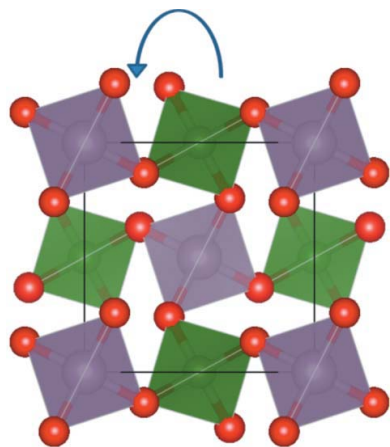
**Supporting information:** this article has supporting information at journals.iucr.org/a

Chemical nomenclature is perceived to be a closed topic. However, this work shows that the identification of polyanionic groups is still ambiguous and so is the nomenclature for some ternary compounds. Two examples, boron phosphate ( $\text{BPO}_4$ ) and boron arsenate ( $\text{BAsO}_4$ ), which were assigned to the large phosphate and arsenate families, respectively, nearly a century ago, are explored. The analyses show that these two compounds should be renamed phosphorus borate ( $\text{PBO}_4$ ) and arsenic borate ( $\text{AsBO}_4$ ). Beyond epistemology, this has pleasing consequences at several levels for the predictive character of chemistry. It paves the way for future work on the possible syntheses of  $\text{SbBO}_4$  and  $\text{BiBO}_4$ , and it also renders previous structure field maps completely predictive, allowing us to foresee the structure and phase transitions of  $\text{NbBO}_4$  and  $\text{TaBO}_4$ . Overall, this work demonstrates that quantum mechanics calculations can contribute to the improvement of current chemical nomenclature. Such revisitation is necessary to classify compounds and understand their properties, leading to the main final aim of a chemist: predicting new compounds, their structures and their transformations.

## 1. Introduction

The part of chemical nomenclature related to the systematic classification of compounds, as introduced by Pauling nearly a century ago, is perceived to be a rather closed topic (Pauling, 1929). In particular, the notation of ternary polycationic  $\text{ABX}_n$  compounds ( $A$  and  $B$  are cations and  $X$  is an anion) was assumed to be that of pseudo-binary  $\text{AX}$  compounds by denoting them as one cation ( $A$ ), and one anion ( $\text{BX}_n$ ). Under this notation,  $\text{ABX}_n$  compounds can be understood as the composition of polyhedral units, formed by  $X$  anions around  $A$  ( $\text{AX}_o$ ) and  $B$  ( $\text{BX}_m$ ) cations. The polyanionic group  $\text{BX}_m$  is usually formed by cation  $B$  with higher valence and smaller coordination, which, according to Pauling's rules, has the stronger electrostatic bond with anion  $X$ . In this way,  $\text{BX}_m$  groups form closed units that tend to separate highly charged  $B$  cations in order to reduce the electrostatic repulsion between these cations (e.g. cyanates or phosphates) (Pauling, 1960).

The rules for naming inorganic compounds were revised in 1970 (IUPAC, 1970), when a non-ambiguous notation was favored over chemical insight. As an example, in classical nomenclature, phosphate represents the polyanion  $\text{PO}_4^{3-}$ , whereas phosphite refers to  $\text{PO}_3^{3-}$ . Within the 1970 IUPAC rules, the term phosphate defines a general negative group with phosphorus as the central atom, irrespective of the oxidation state. However, the existence/recognition of such polyatomic units in complex compounds, without resorting to chemical intuition, may lead to ambiguous cases. Here, we aim



© 2020 International Union of Crystallography

to illustrate one of these cases by analysing in particular  $ABO_4$  compounds containing boron. The natural question lies in how to determine which of the cations should be labeled 'A' and which 'B', *i.e.* which one forms part of the main polyatomic anion. (For clarity, general *B* cations will be noted in italics whereas the boron atom will be noted as a regular capital B.) Historically, several criteria have been proposed to identify these *B* cations: structural similarity, polyhedral compressibility, valence and size are the most important ones. In most  $ABO_4$  compounds with a quartz-related structure (*i.e.* composed of  $AO_4$  and  $BO_4$  tetrahedra), all the criteria above converge. Here we will show that this is not the case for boron-containing compounds.

Understanding the ambient and high-pressure phases of  $ABO_4$  compounds, as well as their behavior under compression, is a challenging task within crystal chemistry, with implications extending to many fields including earth, planetary and materials sciences. Furthermore, since many properties of materials, such as piezoelectricity or thermal expansion, depend on the crystal structure, it becomes imperative to predict the different phases of materials for technological applications (Li *et al.*, 2007). A well known example, owing to its relevance in earth sciences and in different technologies such as radioactive waste recovery, is the family of orthosilicates, which includes the minerals zircon ( $ZrSiO_4$ ) and hafnion ( $HfSiO_4$ ). Many orthosilicates crystallize in the zircon-type structure and undergo a pressure-induced phase transition to the scheelite-type structure. Curiously enough, these compounds can be recovered in the metastable scheelite phase at ambient pressure since they do not revert to the original zircon-type phase upon decompression, thus leading to improved properties for certain applications with respect to the original zircon-type phase (Scott *et al.*, 2001; Liu, 1982).

Predicting the structure of a solid of a given composition at a determined temperature and pressure is of the utmost importance in solid-state science. Until the recent advent of metadynamics and genetic algorithms, the task of predicting the structure of a solid compound was accomplished through trial and error. The consequent use of structure field maps or diagrams was a step in the right direction for design. These maps enable the prediction of the structure of a given compound based on ionic parameters (typically ionic radii). Given the current computational price of predictive algorithms, these maps still play a major role in the prediction of a structure of a compound given its composition, under both ambient conditions and extreme temperature–pressure conditions. Hence, general classifications of compounds in structure field maps or diagrams are crucial when it comes to predicting crystal structure and phase transformations under pressure (*i.e.* their 'reactivity'; Müller & Roy, 1973).

In particular, it is possible to find general trends of  $ABO_4$  compounds in terms of the properties of *A* and *B* cations that enable the prediction of the ambient-pressure structure for a given compound, and its pressure-induced transformations. In this context, diagrams of  $ABO_4$  compounds have usually been constructed by assuming that they are pseudo-binary compounds, formed by  $A^{x+}$  and  $(BO_m)^{x-}$  ions, where the  $BO_m$

group is the polyatomic anion that gives its name to the compound (*e.g.* silicate, phosphate). Once the polyanion is known, the classification is usually done in terms of ionic radii (Dachille & Roy, 1959; Stubican & Roy, 1962; Vorres, 1962; Fukunaga & Yamaoka, 1979; Bastide, 1987; Errandonea & Manjón, 2008; Lashin *et al.*, 2012). Therefore, the identification of the main polyanion is critical to classifying the structural behavior of  $ABO_4$  compounds in order to avoid extensive (and expensive) calculations.

The diagrams for  $ABO_4$  compounds are very rich. Indeed, the large number of cations whose valences sum up to +8 leads to many  $A^xB^{8-x}O_4$  combinations, so the  $ABO_4$  family is large and diverse. In order to simplify their characterization,  $ABO_4$  compounds are divided into subfamilies based on the forming polyanion (Depero & Sangaletti, 1997) (see the supporting information for a brief enumeration). Among these subfamilies (Depero & Sangaletti, 1997), the smallest and least well recognized one (by far) is the orthoborate ( $BO_4$ ) family, whose only known members to date are the very rare minerals of schiavinatoite ( $NbBO_4$ ) and behierite ( $TaBO_4$ ), crystallizing in the zircon-type structure (Zaslavskij & Zvincuk, 1953; Mrose & Rose, 1961; Bayer, 1972; Range *et al.*, 1988; Gramaccioli, 2000; Demartin *et al.*, 2001), as well as possibly  $VBO_4$ , merely referred to as  $BVO_4$  in the work by Müller & Roy (1973). Contrary to expectation, this last compound was not found to be isostructural to silica, and no data have been found about its precise structure (Range *et al.*, 1988). Overall, the orthoborate family of  $ABO_4$  compounds is so poorly understood that the compound  $TaBO_4$  was named  $BTaO_4$  in the work by Fukunaga & Yamaoka (1979), despite the fact it crystallizes in the zircon-type structure (no tantalate is known to crystallize in the zircon-type structure!) and that it was named tantalum borate in previous work (Blasse & Heuvel, 1973). In this context, the omission of the orthoborate subfamily in the first reviews on the systematization of  $ABX_4$  crystal structures and their transformations (Fukunaga & Yamaoka, 1979; Bastide, 1987) is not surprising.

Apart from the schiavinatoite and behierite minerals, and the brief mention of  $BVO_4$ , there are two other boron-containing  $ABO_4$  compounds which have also been known for more than a century (Gramaccioli, 2000): boron phosphate ( $BPO_4$ ) and boron arsenate ( $BAso_4$ ), both crystallizing in the high-cristobalite ( $I\bar{4}$ , No. 82,  $Z = 4$ ) structure (Schulze, 1933). This structure can be viewed as formed by  $PO_4$  ( $AsO_4$ ) and  $BO_4$  polyhedra, which are linked by their corners (Fig. 1). Following Pauling's rules, they were named boron phosphate and boron arsenate, respectively, more than a century ago, owing to the larger valence of P and As (5+) than that of B (3+). In other words,  $PO_4$  and  $AsO_4$  were assumed to be the main polyatomic units. The nomenclature choice was also supported by the structure. Both compounds crystallize in the high-cristobalite structure, which is derived from the  $\alpha$ -quartz structure, comparable to the berlinite structure of aluminium phosphate ( $AlPO_4$ ) and aluminium arsenate ( $AlAsO_4$ ) (Machatschki, 1936; Brill & Debretteville, 1955).

Building upon previous reasoning, the classical nomenclature was also supported by the traditional polyhedral

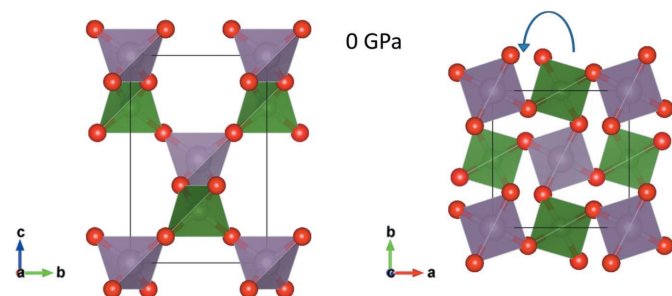


**Figure 1**  
Polyhedral image of  $\text{PBO}_4$  at ambient pressure across the  $bc$  and  $ab$  planes.  $\text{PO}_4$  polyhedra are depicted in green and  $\text{BO}_4$  polyhedra in purple.

compressibility approach in solid-state science. The compressibility of  $\text{ABO}_4$  compounds has usually been summarized in terms of the compressibility of polyhedral units around  $A$  and  $B$  cations (Hazen *et al.*, 1985). It suffices to identify the  $A$  cation as the one that leads to the most compressible polyatomic  $\text{AO}_n$  unit. In this way, the polyhedron  $\text{AO}_n$  governs the compressibility of the material, while the  $\text{BO}_m$  unit is the ‘fixed’ or incompressible polyanion (Hazen & Finger, 1979). When this approach is used for  $\text{BPO}_4$  and  $\text{BaSO}_4$ ,  $\text{PO}_4$  becomes the natural main unit in  $\text{BPO}_4$ , whereas this is doubtful in the case of  $\text{BaSO}_4$  (see Fig. S1 of the supporting information).

All in all, the historical classification of  $\text{BPO}_4$  and  $\text{BaSO}_4$  is substantially supported from all classical pointers except one. The pressure-induced phase transitions observed in these compounds do not match those observed in related phosphates and arsenates, such as  $\text{AlPO}_4$  and  $\text{AlAsO}_4$ . In this context, Fukunaga and Yamaoka’s (FY’s) diagram (Fukunaga & Yamaoka, 1979) provides an extensive rationalization of the ambient phase and pressure-induced phase transitions in  $\text{ABO}_4$  compounds (Fig. 2). This diagram is organized in terms of two variables:  $t = (r_A + r_B)/2r_O$  in the abscissa and  $k = r_A/r_B$  in the ordinate, where  $r_A$ ,  $r_B$  and  $r_O$  are the ionic radii of the  $A$  and  $B$  cations and oxygen, respectively. This diagram enables the prediction of the structure of a given  $\text{ABO}_4$  compound under ambient conditions with good accuracy. Moreover, a ‘south-east’ rule is observed upon pressurization ( $t$  increases,  $k$  decreases), which enables the prediction of structural transformations under pressure assuming that pressure leads to: (i) a greater compression of the oxygen anion over that of the cations and (ii) a greater compression of cation  $A$  over that of cation  $B$ . In FY’s diagram, Pauling’s valence rule is used to decide on the main unit, so that  $A$  cations should have the smaller valence. Since we are comparing boron (3+) with pnictogen ions (5+), the traditional assignment is again supported.

However, this attribution challenges the predictive power of FY’s diagram, which for the first time does not hold for either  $\text{BPO}_4$  or  $\text{BaSO}_4$ . These two compounds undergo a transition at high pressure and high temperature from the high-cristobalite (Haines *et al.*, 2003) to the berlinite (or low-quartz) structure (see the stability region of the quartz-like structure in Fig. 2) (Dachille & Dent Glasser, 1959), *i.e.* they follow an

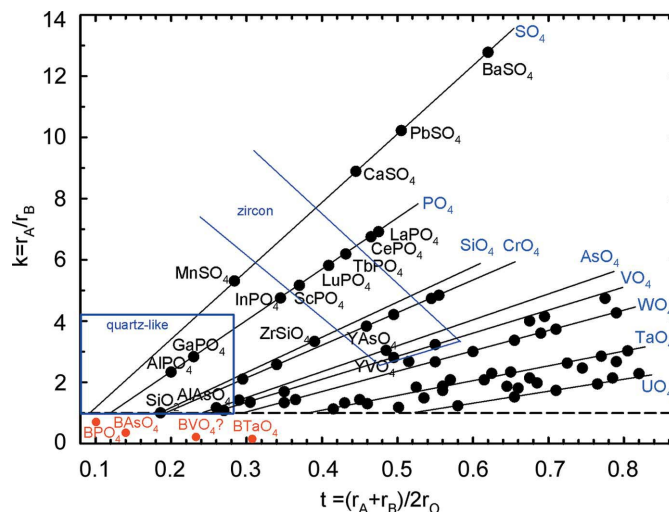


**Figure 2**  
FY’s original diagram with  $\text{BPO}_4$ ,  $\text{BaSO}_4$  and other boron-related compounds (in red) as if they were  $\text{A}^{3+}\text{B}^{5+}\text{O}_4$  compounds, where  $A$  is boron, hence with  $k < 1$ . Clearly, the formulation  $\text{BTaO}_4$  is not compatible with the observed zircon structure under ambient conditions.

anomalous ‘north-east’ behavior in FY’s diagram. It must be stressed that such anomaly would also affect  $\text{BTaO}_4$ , which was already known to be a zircon-type compound (Müller & Roy, 1973), but whose location in FY’s diagram is not compatible with such a structure (see the red symbols and the stability region of the zircon phase in Fig. 2). Finally, it is worth mentioning that the anomaly would also probably affect  $\text{BVO}_4$ , whose structure is unknown (Stubican & Roy, 1962, p. 10). Therefore, it is clear that all boron-containing  $\text{ABO}_4$  compounds call into question the predictive capability of FY’s diagram, both in terms of their structures at ambient pressure and of their pressure-induced phase transitions. For these reasons, the orthoborate subfamily was not allocated in FY’s original diagram (Fukunaga & Yamaoka, 1979). Only  $\text{BPO}_4$  and  $\text{BaSO}_4$ , two well known compounds, were allocated in this diagram, assuming they were a phosphate and an arsenate, respectively, and their anomalous pressure-induced phase transitions were barely discussed in the work.

The anomaly of  $\text{BPO}_4$  and  $\text{BaSO}_4$  was noted by Bastide (1987) who, following the initiative of Dachille & Roy (1959), classified  $\text{ABO}_4$  compounds using the cation and anion sizes as the main criterion. Taking into account the smaller ionic radius (Shannon, 1976) of B (0.11 Å) as opposed to those of P (0.17 Å) and As (0.34 Å), Bastide renamed these two compounds  $\text{PBO}_4$  and  $\text{AsBO}_4$  (Bastide, 1987). He suggested that the predictive power of FY’s diagram could be recovered if the argument used to identify cations  $A$  and  $B$  in  $\text{ABO}_4$  compounds was size rather than valence. Under this characterization, all anomalies of boron-based compounds could be solved. However, a definitive justification for this change in the chemical nomenclature was still missing.

In this work we resort to the topology of the electron density in order to justify this choice. The big technical improvements in high-pressure experiments have resulted in the ability to accurately resolve many high-pressure solid structures. Simultaneously, improvement in computational

methods and power has led to important improvements in their interpretations. The topological analysis of the electron density, the electron-density Laplacian and the electron localization function have led to numerous advances in the microscopic understanding of crystal properties in the fields of mineralogy and geosciences. Ormeci and Rosner were able to explain the high total energy of the Sb high-pressure structure due to the lack of chemical bonding between the chain atoms (Ormeci & Rosner, 2004). It has also been possible to associate the location of the proton-docking sites determined in several silica polymorphs by Fourier transform infrared spectroscopy studies with the vicinity of the electron lone pairs (Gibbs *et al.*, 2003).

Through this contribution, we follow this direction and show, by means of *ab initio* total-energy calculations and topology, that BPO<sub>4</sub> and BAsO<sub>4</sub> are borates, solving an almost century-old controversy. Therefore, they will be denoted by PBO<sub>4</sub> and AsBO<sub>4</sub> from now on. Moreover, we provide a mathematical foundation in terms of chemical hardness for the use of a size criterion over valence and also over polyhedral compressibility in ABO<sub>4</sub> compounds. This result has important implications in solid-state science, where the polyhedral compressibility approach is still widely used. As an example of the usefulness of our approach, a new version of FY's diagram, where the new borates follow the main trends, is provided. More generally, our approach lays the foundations for the use of quantum mechanics calculations as a source of information that can be used to settle arguments in which common chemical approaches (size, valence, electronegativity *etc.*) lead to different answers.

## 2. Methods

Electronic structure calculations were carried out within the density functional theory (DFT) formalism with a plane-wave pseudopotential approach, as implemented in the Vienna *ab initio* simulation package (VASP). We used the Perdew–Burke–Ernzerhof generalized gradient approximation (GGA-PBE) for the exchange–correlation functional (Perdew *et al.*, 1996), and the projector augmented wave (PAW) all-electron description of the electron–ion-core interaction (Kresse & Joubert, 1999). Brillouin-zone integrals were approximated using the Monkhorst–Pack method (Monkhorst & Pack, 1976), and the energies converged with respect to *k*-point density (*k*-point grid spacing of  $2\pi \times 0.03 \text{ \AA}^{-1}$ ) and to the plane wave kinetic energy cut-off (600 eV).

Identifying the main unit of a solid from its wavefunction requires obtaining atomic contributions and the bonding pattern. This can be achieved by resorting to the electron density in the framework of the dynamical system theory (Alinger *et al.*, 1998; Bader, 1994; Abraham & Marsden, 1994). This approach was developed by Bader and co-workers in what is known as the Quantum Theory of Atoms In Molecules (QTAIM) (Bader, 1990). The electron density presents a rich topology with mountains, valleys, plateau zones and different types of critical points (maxima, saddle, ring and cage points) where  $\nabla\rho(r)$  vanishes. Within QTAIM, the first-order saddle

points are indicative of the bonding between two atoms, which leads to them being called ‘bond critical points’ (b.c.p.'s). Zero-flux surfaces of the  $\nabla\rho(r)$  enclose 3D regions that can be associated with atoms (also known as the basins). In the case of crystals, this partition leads to basins that are finite, disjoint and space filling, which means the addition of all of them over the unit cell recovers its full unit-cell volume. In this way, this non-overlapping and filling partition allows us to study the very interesting properties of crystalline materials. Among the achievements of QTAIM, we may outline the identification of the ‘nature’ of functional groups and the transferability of their properties from one system to another. Currently, QTAIM is being used by both theoreticians and experimentalists in fields ranging from solid-state physics and X-ray crystallography to drug design and biochemistry. For a good overview of its applications, we refer readers to the work of Boyd & Matta (2007).

For each structure, the geometry was optimized at several pressures. The pressure–volume data were used to evaluate the corresponding equation of state (EOS) parameters. The equilibrium volume ( $V_0$ ) is straightforward to obtain whereas the bulk modulus ( $B_0$ ) and its first pressure derivative ( $B'_0$ ) were obtained after fitting the theoretical unit-cell volume versus pressure data to the analytical Vinet EOS (Vinet *et al.*, 1986). Polyhedral volumes were obtained with the program VESTA and also adjusted to the Vinet EOS to obtain polyhedral compressibilities. The topological analysis of the electron density in crystals within the QTAIM approach was carried out using the CRITIC code, which takes information on the electron density obtained by *ab initio* calculations from CHGCAR files from the program VASP (Otero-de-la-Roza *et al.*, 2009, 2012). Basin volumes ( $v_i$ ) and charges ( $q_i$ ) were calculated by integrating the corresponding density operators. We checked the performance of the partition by assessing the recovery of the unit-cell volume.

The concept of chemical hardness, as defined in conceptual DFT, is also used here. Indeed, the chemical hardness (Geerlings *et al.*, 2003) is given by the second derivative of the energy,  $E$ , with respect to the number of electrons,  $N$ , at constant chemical potential,  $\nu$  (*i.e.* at a fixed geometry in our case):

$$\eta = \left( \frac{\partial^2 E}{\partial N^2} \right)_\nu = E_{\text{gap}}.$$

In solids, this quantity yields the band gap,  $E_{\text{gap}}$ . This quantity can be related to the atomic compressibility,  $\kappa_i$ , as follows (Yang *et al.*, 1987):

$$\kappa_i = \frac{V}{\eta_i M^2}. \quad (1)$$

This equation establishes a link between a microscopic parameter-dictating reactivity (*i.e.* chemical hardness, or  $\eta$ ) and the macroscopic resistance of the solid to external pressures for an atomic solid, with  $M$  atoms in the unit cell.

This is important because it makes it possible to relate compressibility to the shape and size of the atoms. Indeed, it has been demonstrated that a basic relationship between the



**Table 1**

Cell parameters for  $\text{PBO}_4$  and  $\text{AsBO}_4$  from our calculations and previous experimental results (Haines *et al.*, 2003).

The cell parameter  $a$  is given in Å and  $B_0$  in GPa.

	$\text{PBO}_4$					$\text{AsBO}_4$				
	$a$	$c/a$	$x$	$B_0$	$B'_0$	$a$	$c/a$	$x$	$B_0$	$B'_0$
Theory	4.433	1.513	0.132	53.7	4.2	5.584	1.499	0.155	49.5	3.7
Experiment	4.339	1.531	0.140	56.0	4.7	4.467	1.526	0.158	49.0	5.0

chemical hardness of an atom ( $\eta_i$ ) and its size ( $r_i$ ) holds (Gázquez & Ortiz, 1984):

$$\eta_i = -\frac{1}{4r_i}. \quad (2)$$

Putting equations (1) and (2) together, we can see that, in agreement with common chemical knowledge, atomic compressibility is proportional to atomic size ( $\kappa_i \propto r_i$ ), meaning that ions become softer as their radius increases.

### 3. Results and discussion

The high-cristobalite structure of  $\text{PBO}_4$  ( $\text{AsBO}_4$ ) is derived from the ideal tetragonal cristobalite structure by a tilting of the polyhedra (see the arrow in Fig. 1) around the twofold axes parallel to the  $c$  axis (O'Keeffe & Hyde, 1976; Léger *et al.*, 2001). This tilting leads to a departure of the  $c/a$  axial ratio and the  $x$  position of the O atoms ( $x_O$ ) from their ideal values in the cristobalite structure ( $c/a = \sqrt{2}$ ,  $x_O = 0$ ; see Table 1). Our calculated values of structural parameters for both  $\text{PBO}_4$  and  $\text{AsBO}_4$  under compression are in rather good agreement with previous experimental and theoretical values and allow conclusions to be drawn on the behavior under pressure (Haines *et al.*, 2003) (see Figs. S2–S5). Notably, our theoretical data yield a bulk modulus of 53.7 GPa (49.5 GPa) for  $\text{PBO}_4$  ( $\text{AsBO}_4$ ), which is in good agreement with the experimental values of 56.0 GPa (49.0 GPa) (Haines *et al.*, 2003).

Of special interest are the results for  $x_O$ , since this parameter is related to the average tilting angle  $\phi$  (Haines *et al.*, 2003; O'Keeffe & Hyde, 1976):

$$\phi = \arctan[4x_O]. \quad (3)$$

Unlike many  $\text{ABO}_4$  compounds, the low-pressure compressibility of the high-cristobalite structure of  $\text{PBO}_4$  and  $\text{AsBO}_4$  is not related to polyhedral compression, but rather to the increase of the tilting angle of the constituent polyhedral units [Fig. 3(a)]. This process results in a collapse of the structural gaps of the  $ab$  plane upon pressurization (see movie of the compression mechanism available in the supporting information). In particular, the highly anisotropic  $c/a$  compressibility of  $\text{AsBO}_4$  [Fig. 3(b)] has been related to the increased tilting (Haines *et al.*, 2003). However, our calculations show that the evolution of the tilting is homogenous for both compounds, meaning that it does not explain the different trends in the  $c/a$  ratio observed under compression in  $\text{AsBO}_4$  (which are not observed in  $\text{PBO}_4$ ).

**Table 2**

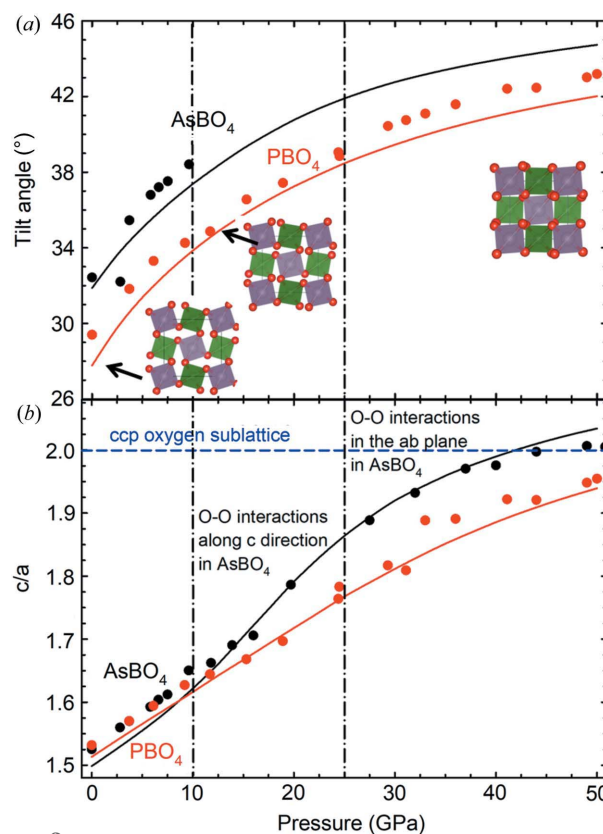
$B_0$  values (in GPa) for polyhedral units.

X represents P/As. Both atomic and void polyhedra are included. T stands for tetrahedron and Oh for octahedral void.

Polyhedron	$\text{BO}_4$	$\text{XO}_4$	Void T1	Void T2	Void T3	Void T4	Void Oh
$\text{PBO}_4$	298.0	648.7	24.20	25.94	107.31	105.30	49.94
$\text{AsBO}_4$	251.8	519.0	21.99	26.17	73.24	71.12	45.41

Following previous studies on the change of polarity of  $\text{BPO}_4$  under pressure (Mori-Sánchez *et al.*, 2001), we reviewed the evolution of atomic charges under pressure, but no major changes were found (Fig. S6). Instead, our analysis of the electron density showed that tilting results in significant changes in the bonding pattern (see *Methods*), which, in turn, affects the compressibility of the structure. Therefore, the greater size of As relative to P makes the As atom more receptive to these contact changes (see the relative atomic volumes in Table 2).

At 0 GPa, common O–As and O–B bonds are observed in Fig. 4(a), where the expected  $\text{AsO}_4$  and  $\text{BO}_4$  polyhedra are highlighted. Notably, new O–O contacts appear between oxygen atoms belonging to different layers at 10 GPa

**Figure 3**

(a) Pressure dependence of polyhedra tilting in  $\text{PBO}_4$  (red) and  $\text{AsBO}_4$  (black) as calculated from equation (1). Tilting is shown in the polyhedral representation for some representative pressures. (b) Evolution of the  $c/a$  ratio upon pressurization of  $\text{PBO}_4$  (red) and  $\text{AsBO}_4$  (black). Theoretical data (lines) are compared with experimental data (symbols) from the work by Haines *et al.* (2003). Bonding regions are marked with vertical lines and labeled accordingly in the insets.

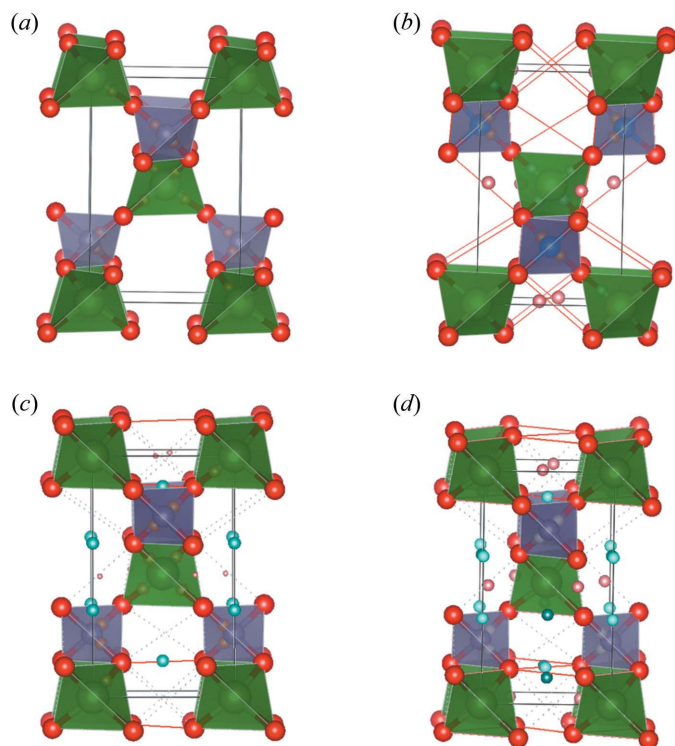


**Figure 4**  
Evolution of bond critical points (b.c.p.'s) in compressed  $\text{AsBO}_4$  at (a) 0 GPa, (b) 10 GPa, (c) 15 GPa and (d) 22 GPa. Oxygen in red, As in green and B in purple. B.c.p.'s are represented with small spheres: O—As and O—B bonds at 0 GPa (in orange), O—O bonds at 10 GPa (pink), interlayer bonds at 15 GPa (blue) and 22 GPa (green). Polyhedra have been colored in blue ( $\text{BO}_4$ ) and green ( $\text{AsO}_4$ ) at 0 GPa to facilitate differentiation of As—O and B—O bonds.

[Fig. 4(b)]. These contacts occur between the rotating units, such that the  $c/a$  ratio is only slightly affected. Moreover, new O—O contacts of O atoms in the same  $ab$  plane are observed above 15 GPa [Fig. 4(c)] and again at 22 GPa [Fig. 4(d)]. From a chemical point of view, the new bonds correspond to  $\text{O}^{2-}$  polymerization. These O links hinder the tilting, thus explaining the anisotropic behavior of  $\text{AsBO}_4$ . This new set of bonds in turn decreases the compressibility of  $c$ , leading to a plateau in the  $c/a$  plot. In summary, the analysis of the electron density permits the explanation of the anisotropic behavior of the high-cristobalite structure of  $\text{AsBO}_4$  as the result of the polymerization of oxygen atoms upon pressurization.

We can also use the information obtained from the electron density to resolve the controversy about the nomenclature of  $\text{PBO}_4$  and  $\text{AsBO}_4$ . As discussed above, FY's diagram is a good structure field map for describing and predicting the behavior of  $\text{ABO}_4$  compounds, except in the case of boron-based compounds (see Fig. 2). The latter constitute a rare case, in which valence and size give different answers for the designation of  $A$  and  $B$  cations; in other words, the choice of the main polyatomic  $\text{BO}_4$  unit in these materials becomes crucial. We argue that following Bastide's initiative (Bastide, 1987), size constitutes a better criterion than valence. In such a case,  $\text{BPO}_4$  and  $\text{BaSO}_4$  with  $k < 1$  will become  $\text{PBO}_4$  and  $\text{AsBO}_4$

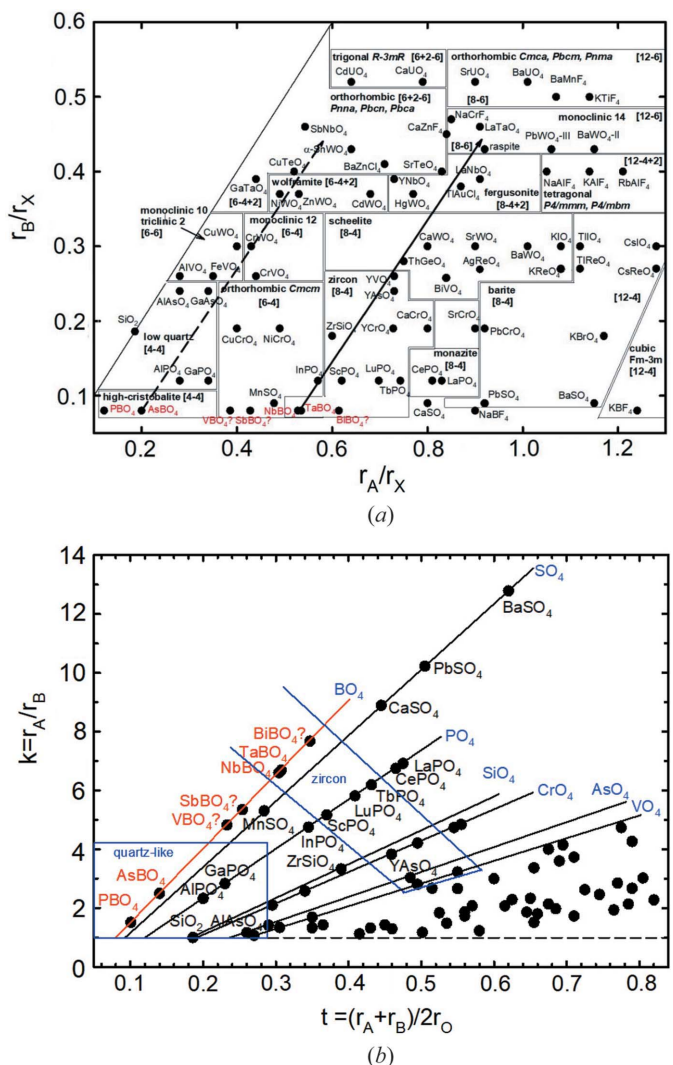


**Figure 5**  
(a) Bastide's diagram for  $ABO_4$  compounds. The whole family of borates is indicated in red. (b) Corrected FY's diagram with  $PbO_4$  and  $AsBO_4$  re-allocated by considering that both are borates. The family of borates is highlighted in red.

with  $k > 1$ , and their phase transition will follow the south-east rule, like all other  $ABO_4$  compounds in FY's diagram [compare Figs. 5(a) and 5(b)].

The south-east rule in FY's diagram implies that cation *A* compresses faster than cation *B*. It is the effect of this rule on *k* that accounts for the failure of the boron compounds to reproduce the general behavior. Hence, the crucial factor in the classification of these compounds is the compression rate of the *A* and *B* cations. Historically, this was checked by means of the polyhedral approach explained above. However, in the case of compounds such as PBO<sub>4</sub> and AsBO<sub>4</sub>, whose main compression mechanism is tilting, this approach is inadequate, meaning that the compressibility of these compounds is not related to the compressibility of atomic polyhedra, but to the compression of the voids between them (Fig. 3). In order to prove this, we calculated the evolution of the tetrahedral (T) and octahedral (Oh) voids in the high-cristobalite structure upon pressurization (see Table 2 and Fig. S7). It can be seen

**Table 3**  
Atomic bulk moduli  $B_{0i}$  (in GPa) as determined from QTAIM.

Atom $i$	PBO <sub>4</sub>		AsBO <sub>4</sub>	
	$B_{0i}$	$f_i$	$B_{0i}$	$f_i$
O	48.0	0.785	42.0	0.862
P/As	117.5	0.172	98.5	0.118
B	150.9	0.043	128.3	0.019

that it is precisely these void units, not attributable to any given atom within the polyhedral approach, which are mainly responsible for the compression of the high-cristobalite structure of both PBO<sub>4</sub> and AsBO<sub>4</sub>. Note that the compressibility of the voids in PBO<sub>4</sub> (AsBO<sub>4</sub>) is more similar to that of the bulk than those of the BO<sub>4</sub> and PO<sub>4</sub> (AsO<sub>4</sub>) units, whose relative volume decrease is less than 10%, up to 50 GPa. Hence, we can see the historical polyhedral approach is not valid for rationalizing the behavior of structures with voids, such as the high-cristobalite structures of PBO<sub>4</sub> and AsBO<sub>4</sub>.

In order to generalize the size concept in FY's and Bastide's diagrams, a definition of atomic volumes without voids is needed. Such a definition is provided by the atomic partition introduced by the topological analysis of the electron density within QTAIM. This approach associates the region around each atom to each nucleus, just as a mountain is represented by its summit. This provides a finite basin volume  $\Omega_i$  to each atom  $i$ , which results in no voids left in the structure because the sum of all  $\Omega_i$  results in the total unit-cell volume. Using this definition of atomic volumes, the macroscopic compressibility of the crystal can be expressed as a sum of atomic contributions, as follows:

$$\kappa = -\frac{1}{V} \frac{\partial V}{\partial P} = \sum f_i \kappa_i, \quad (4)$$

where  $\kappa_i$  defines the atomic compressibility and  $f_i = V_i/V$  is the fractional occupation volume of the  $i$ th atom (of volume  $V_i$ ) in the unit cell of volume  $V$  (Martin Pendás *et al.*, 2000; Recio *et al.*, 2001). Under this representation, not only are basin volumes and charge populations additive, but also compressibilities. It should be noted that this definition of atomic compressibility is applicable to other non-overlapping partitions that fill the whole volume (*e.g.* Voronoi).

The evolution upon compression of the volume of the QTAIM atomic basins  $\Omega_i$  for P (As), B and O in the high-cristobalite structure of PBO<sub>4</sub> (AsBO<sub>4</sub>) is shown in Fig. S8. Furthermore, atomic bulk moduli have been calculated following equation (4) from a Vinet fit, leading to the data collected in Table 3. It can be observed that the largest compressibility (largest slope) corresponds to the O atom, while the smallest compressibility (smallest slope) corresponds to the B atom. Consequently, electron-density-derived volumes within QTAIM clearly indicate that the compressibility of the B atom is much smaller than that of the P and As atoms, thus suggesting that boron must be the *B* atom in boron-containing *ABO*<sub>4</sub> compounds. This result also points to the relevance of electron-density studies in solid-state science,

as already highlighted in the growing field of quantum crystallography (Genoni *et al.*, 2018).

In summary, the QTAIM approach yields the ability to discern the hardest atom and, as a result, find the main polyatomic unit. It does, however, have the disadvantage of requiring the calculation of the EOS for every atomic contribution, which can be cumbersome. Fortunately, we can design several layers of approximations to circumvent this. Looking back at equation (4), the contribution of an ion to the total compressibility will depend on its relative volume in the cell  $d_i$ , but also on its compressibility  $\kappa_i$ . It has been shown in equation (1) that hydrostatic compressibility of atom  $i$  is inversely proportional to the hardness  $\eta_i$  (see *Methods* for further details) (Yang *et al.*, 1987).

This equation establishes a link between a microscopic parameter-dictating reactivity (*i.e.* chemical hardness, or  $\eta$ ) and the resistance of the solid to external pressures. This is important because it allows us to relate compressibility to the shape and size of the atoms. Indeed, it has been demonstrated that hardness is inversely proportional to atomic size (Gázquez & Ortiz, 1984). Putting these concepts together (see *Methods* for a complete derivation), we can see that, in agreement with common chemical knowledge, atomic compressibility is proportional to atomic size ( $\kappa_i \propto r_i$ ). In other words, according to common acceptance, ions become softer as their radius increases. Fig. S9 shows that this relationship holds for all the different ions in PBO<sub>4</sub> and AsBO<sub>4</sub>. Although here we have used atomic radii derived from the partition of the unit-cell volume in a solid within QTAIM [assuming a spherical approximation,  $r_{\text{QTAIM}} = 3V^{1/3}/(4\pi)$ ], the relationship can also be used with Shannon ionic radii. In summary, this method provides a workhorse approximation in order to determine *a priori* the hard ions in a crystal, and hence the polyanion complex. Furthermore, we have provided the physical foundation for the prevalence of size over valence that should dictate the attribution of *A* and *B* cations in *ABO*<sub>4</sub> compounds. Consequently, the nomenclature of these compounds should be guided by size, simultaneously restoring the predictive character of structure field maps.

We want to highlight that all the results reported here for PBO<sub>4</sub> and AsBO<sub>4</sub> have several consequences from a chemical point of view. First and foremost, the BO<sub>4</sub> units (including their corresponding structural voids) are the less compressible ones; therefore, they can be considered as the main structural polyatomic units of these two pseudo-binary compounds. Second, these two compounds should be considered borates and not a phosphate and an arsenate, respectively, as was previously assumed. In other words, the notation according to their properties should be PBO<sub>4</sub> and AsBO<sub>4</sub> instead of BPO<sub>4</sub> and BAsO<sub>4</sub>, respectively.

From a high-pressure point of view, the fact that the bulk moduli are proportional to size [equations (1)–(3)] confirms the use of ionic radii as a good approximation for classifying polyatomic anions and ensuring coherent nomenclature in ambiguous cases. We propose the use of the larger ionic radius when choosing the *A* cation in *ABO*<sub>4</sub> compounds within FY's diagram, as done in Bastide's diagram. Hence, all *ABO*<sub>4</sub>



compounds in FY's diagram must have  $k > 1$ . This would lead to the reallocation of both  $\text{PBO}_4$  and  $\text{AsBO}_4$  in the revised FY's diagram [Fig. 5(b)] and the use of the 'south-east' rule for understanding pressure-induced phase transitions in all  $\text{ABO}_4$  compounds.

Most importantly, this redefinition of FY's diagram reinforces its predictive power even for unknown phases. This ensures a low-cost understanding of new phases and their transformations, which we can now test. In particular, if the very rare zircon-type minerals schiavinitoite ( $\text{NbBO}_4$ ) and behierite ( $\text{TaBO}_4$ ) are considered as borates, the orthoborate subfamily is further enlarged. According to the corrected version of FY's diagram, as well as Bastide's diagram,  $\text{NbBO}_4$  and  $\text{TaBO}_4$  should crystallize in the zircon structure and transform under pressure to either the scheelite or the monazite phase. Testing this hypothesis with our calculations on the three phases, we can conclude that, at zero pressure, the zircon-type structure is indeed more stable than the scheelite and monazite phases. Moreover, we predict a pressure-induced phase transition from the zircon structure towards the scheelite phase (see Fig. S10) at 47.5 GPa (52.0 GPa) for  $\text{NbBO}_4$  ( $\text{TaBO}_4$ ). It is important to remark that the orthoborate family of  $\text{ABO}_4$  compounds is the only one featuring the  $A$  cation with a greater valence (+5) than the  $B$  cation (+3).

In addition, the redefinition of the chemical nomenclature of  $\text{PBO}_4$  and  $\text{AsBO}_4$  creates the opportunity for exploring interesting new avenues. It opens the door for the possible synthesis of other  $\text{ABO}_4$  compounds with  $A$  atoms from the 5B group (Sb, Bi). According to the corrected versions of FY's and Bastide's diagrams,  $\text{SbBO}_4$  and  $\text{BiBO}_4$  should crystallize in the compact orthorhombic  $Cmcm$  and tetragonal zircon-type structures, respectively, and the yet unknown structure of  $\text{VBO}_4$  could also have  $Cmcm$  symmetry (see Fig. 5).

#### 4. Conclusions

We have shown, by means of an analysis of the electron density provided by quantum mechanics calculations, that the chemical nomenclature of pseudo-binary compounds, like the  $\text{ABO}_4$  ones, is not yet a solved issue. Until now, the identification of polyatomic anions relied on chemical knowledge and, in most cases, the analysis of the valence and size of the atoms provided a mutually coherent answer. What we have shown instead is that, in boron-containing  $\text{ABO}_4$  compounds like  $\text{PBO}_4$  and  $\text{AsBO}_4$ , this is not the case. Boron ( $\chi = 2.04$ , Pauling scale) has a similar electronegativity to that of phosphorus ( $\chi = 2.19$ ) and arsenic ( $\chi = 2.18$ ). Phosphorus and arsenic hold a higher valence (+5) than boron (+3), which usually leads to harder anions. However, the small size of boron ( $r_B = 0.11$ ,  $r_P = 0.17$  and  $r_{As} = 0.34 \text{ \AA}$ ) leads to an important competition. In fact, the chemical hardness of these ions at their formal charge is largely more important for  $\text{B}^{3+}$  ( $\eta_{\text{B}^{3+}} = 221$ ,  $\eta_{\text{P}^{5+}} = 155$  and  $\eta_{\text{As}^{5+}} = 65 \text{ eV}$ ) despite its smaller valence. Consequently, our calculations show that boron must be the  $B$  cation in boron-containing  $\text{ABO}_4$  compounds.

Our results have important implications for general chemistry and solid-state sciences. (i) The two compounds need to be renamed phosphorus borate ( $\text{PBO}_4$ ) and arsenic borate ( $\text{AsBO}_4$ ) – nomenclature that is in agreement with their properties. We must emphasize that this result prompts the revision of the nomenclature of borophosphates, which perhaps should be renamed as phosphoroborates (Kniep *et al.*, 1994). (ii) This would mean that the general FY's diagram of  $\text{ABO}_4$  compounds should be reformulated in terms of size instead of valence, in order to be able to welcome novel structures while keeping its predictive power. In this way, both FY's and Bastide's diagrams for  $\text{ABO}_4$  compounds are defined on the same basis. (iii) The new borates  $\text{PBO}_4$  and  $\text{AsBO}_4$  form – together with  $\text{NbBO}_4$ ,  $\text{TaBO}_4$  and the poorly known  $\text{VBO}_4$  – the orthoborate subfamily, *i.e.* the only  $\text{ABO}_4$  compounds with the  $A$  cations having a valence higher than +4; this could also mean that zircon-type borates could be the most incompressible  $\text{ABO}_4$  compounds, owing to the well known relationship between the bulk modulus and the formal charge of the  $A$  cation in zircon-type compounds (Errandonea & Manjón, 2008; Brill & Debretville, 1955). (iv) The existence of  $\text{PBO}_4$  and  $\text{AsBO}_4$  opens the door for the synthesis of new members of the borate family with  $A$  cations of a +5 valence, such as the yet unknown  $\text{SbBO}_4$  and  $\text{BiBO}_4$  compounds.

Finally, from a more general perspective we can draw two main conclusions. With respect to chemistry, the nomenclature of compounds is still an open topic and quantum mechanics calculations, together with electron-density analysis, can help us to improve it. More specifically, this is another example where QTAIM is a powerful tool for understanding crystal properties. As an example, Zhang *et al.* were recently able to explain the isotropic thermoelectric properties of  $\text{Mg}_3\text{Sb}_2$  from the bonding network (Zhang *et al.*, 2018). In our case, we have highlighted the need to resort to QTAIM for the identification of the main polyanions in ternary systems, which still remain defined in terms of chemical intuition. Resorting to a general rationalization in terms of properties, these ambiguities can be solved when characteristics such as valence or size do not run in the same direction. In relation to physics, the historical polyhedral approach has been shown to be invalid for rationalizing the behavior of structures with voids under compression, like the high-crystallite structure. In these cases, the analysis of electron density can facilitate the definition of extended concepts. As an example, Rahm *et al.* have recently redefined electronegativity, leading to a scale similar to Allen's (Rahm *et al.*, 2019). Here, we have shown that the use of QTAIM atomic volumes enables recovery of the predicting capability of structure field maps.

#### Acknowledgements

We especially acknowledge the availability of experimental data for  $\text{PBO}_4$  and  $\text{AsBO}_4$  kindly provided by J. Haines (Haines *et al.*, 2003), and the discussions with Dr J. A. Sans.

## Funding information

This research was partially supported by Spanish MINECO (grant Nos. MAT2015-71070-REDC and MAT2016-75586-C4-2-P, and MALTA Consolider Team RED2018-102612-T) and Generalitat Valenciana (grant No. PROMETEO/2018/123-EFIMAT). J. Contreras-García thanks CALSIMLAB (public grant No. ANR-11-LABX-0037-01), overseen by the French National Research Agency (ANR) as part of the Investissements d'Avenir program (grant No. ANR-11-IDEX-0004-02). M. Marqués acknowledges support from the ERC grant 'Hecate' and computational resources provided by the UKCP consortium under EPSRC grant EP/P022561/1.

## References

- Abraham, R. H. & Marsden, J. E. (1994). *Foundations of Mechanics*. Reading: Addison Wesley.
- Alinger, N. L., Clark, T., Gasteiger, J., Kollman, P. A., Schaefer, H. F. III, Schreiner, P. R. & Schleyer, von R. (1998). *Encyclopedia of Computational Chemistry*, edited by R. F. W. Bader. Chichester: Wiley.
- Bader, R. F. W. (1990). *Atoms in Molecules, a Quantum Theory*. Oxford: Clarendon.
- Bader, R. F. W. (1994). *Phys. Rev. B*, **49**, 13348–13356.
- Bastide, J. P. (1987). *J. Solid State Chem.* **71**, 115–120.
- Bayer, G. (1972). *J. Less-Common Met.* **26**, 255–262.
- Blasse, G. & Van Den Heuvel, G. P. M. (1973). *Phys. Status Solidi A*, **19**, 111–117.
- Boyd, R. J. & Matta, C. F. (2007). Editors. *The Quantum Theory of Atoms in Molecules. From Solid State to DNA and Drug Design*. Weinheim: Wiley-VCH.
- Brill, R. & Debretteville, A. P. (1955). *Acta Cryst.* **8**, 567–570.
- Dachille, F. & Dent Glasser, L. S. (1959). *Acta Cryst.* **12**, 820–821.
- Dachille, F. & Roy, R. (1959). *Z. Kristallogr.* **111**, 451–461.
- Demartin, F., Diella, V., Gramaccioli, C. M. & Pezzotta, F. (2001). *Eur. J. Mineral.* **13**, 159–165.
- Depero, L. E. & Sangaletti, L. (1997). *J. Solid State Chem.* **129**, 82–91.
- Errandonea, D. & Manjón, F. J. (2008). *Prog. Mater. Sci.* **53**, 711–773.
- Fukunaga, O. & Yamaoka, S. (1979). *Phys. Chem. Miner.* **5**, 167–177.
- Gázquez, J. L. & Ortiz, E. (1984). *J. Chem. Phys.* **81**, 2741–2748.
- Geerlings, P., De Proft, F. & Langenaeker, W. (2003). *Chem. Rev.* **103**, 1793–1873.
- Genoni, A., Bučinský, L., Claiser, N., Contreras-García, J., Dittrich, B., Dominiak, P. M., Espinosa, E., Gatti, C., Giannozzi, P., Gillet, J. M., Jayatilaka, D., Macchi, P., Madsen, A. Ø., Massa, L., Matta, C. F., Merz, K. M., Nakashima, P. N. H., Ott, H., Ryde, U., Schwarz, K., Sierka, M. & Grabowsky, S. (2018). *Chem. Eur. J.* **24**, 10881–10905.
- Gibbs, G. V., Cox, D. F., Boisen, M. B. Jr, Downs, R. T. & Ross, N. L. (2003). *Phys. Chem. Miner.* **30**, 305–316.
- Gramaccioli, C. M. (2000). *R. Fis. Acc. Lincei*, **11**, 197–199.
- Haines, J., Chateau, C., Léger, J. M., Bogicevic, C., Hull, S., Klug, D. D. & Tse, J. S. (2003). *Phys. Rev. Lett.* **91**, 015503.
- Hazen, R. M. & Finger, L. W. (1979). *J. Geophys. Res.* **84**, 6723–6728.
- Hazen, R. M., Finger, L. W. & Mariathasan, J. W. E. (1985). *J. Phys. Chem. Solids*, **46**, 253–263.
- IUPAC (1970). *Nomenclature of Inorganic Solids. Definitive Rules*. 3rd ed. London: International Union of Pure and Applied Chemistry.
- Kniep, R., Gözel, G., Eisenmann, B., Röhr, C., Asbrand, M. & Kizilyalli, M. (1994). *Angew. Chem. Int. Ed. Engl.* **33**, 749–751.
- Kresse, G. & Joubert, D. (1999). *Phys. Rev. B*, **59**, 1758–1775.
- Lashin, V. E., Khritokhin, N. A. & Andreev, O. V. (2012). *Russ. J. Inorg. Chem.* **57**, 1584–1587.
- Léger, J. M., Haines, J., Chateau, C., Bocquillon, G., Schmidt, M. W., Hull, S., Gorelli, F., Lesauze, A. & Marchand, R. (2001). *Phys. Chem. Miner.* **28**, 388–398.
- Li, H., Zhou, S. & Zhang, S. (2007). *J. Solid State Chem.* **180**, 599–605.
- Liu, L. G. (1982). *Earth Planet. Sci. Lett.* **57**, 110–116.
- Machatschki, F. (1936). *Z. Krist.* **94**, 222.
- Martín Pendás, A., Costales, A., Blanco, M. A., Recio, J. M. & Luaña, V. (2000). *Phys. Rev. B*, **62**, 13970–13978.
- Monkhorst, H. J. & Pack, J. D. (1976). *Phys. Rev. B*, **13**, 5188–5192.
- Mori-Sánchez, P., Pendás, A. M. & Luaña, V. (2001). *Phys. Rev. B*, **63**, 125103.
- Morse, M. E. & Rose, W. J. (1961). *Am. Min. Soc. Prog. A*, 111A.
- Müller, O. & Roy, R. (1973). *Z. Kristallogr.* **138**, 237–253.
- O'Keeffe, M. & Hyde, B. G. (1976). *Acta Cryst.* **B32**, 2923–2936.
- Ormeci, A. & Rosner, H. (2004). *Z. Kristallogr.* **219**, 370–375.
- Otero-de-la-Roza, A., Blanco, M. A., Pendás, A. M. & Luaña, V. (2009). *Comput. Phys. Commun.* **180**, 157–166.
- Otero-de-la-Roza, A., Johnson, E. R. & Contreras-García, J. (2012). *Phys. Chem. Chem. Phys.* **14**, 12165–12172.
- Pauling, L. (1929). *J. Am. Chem. Soc.* **51**, 1010–1026.
- Pauling, L. (1960). *The Nature of the Chemical Bond and the Structure of Molecules and Crystals: An Introduction to Modern Structural Chemistry*, 3rd ed., pp. 543–562. Ithaca: Cornell University Press.
- Perdew, J. P., Burke, K. & Ernzerhof, M. (1996). *Phys. Rev. Lett.* **77**, 3865–3868.
- Rahm, M., Zeng, T. & Hoffmann, R. (2019). *J. Am. Chem. Soc.* **141**, 342–351.
- Range, K. J., Wildenauer, M. & Heyns, A. M. (1988). *Angew. Chem. Int. Ed. Engl.* **27**, 969–971.
- Recio, J. M., Franco, R., Martín Pendás, A., Blanco, M. A., Pueyo, L. & Pandey, R. (2001). *Phys. Rev. B*, **63**, 184101.
- Schulze, G. E. (1933). *Naturwissenschaften*, **21**, 562.
- Scott, H. P., Williams, Q. & Knittle, E. (2001). *Phys. Rev. Lett.* **88**, 015506.
- Shannon, R. D. (1976). *Acta Cryst.* **A32**, 751–767.
- Stubican, V. V. & Roy, R. (1962). *Z. Kristallogr.* **119**, 90–97.
- Vinet, P., Ferrante, J., Smith, J. R. & Rose, J. H. (1986). *J. Phys. C: Solid State Phys. L*, **19**, 467.
- Vorres, K. S. (1962). *J. Chem. Educ.* **39**, 566.
- Yang, W., Parr, R. G. & Uytterhoeven, L. (1987). *Phys. Chem. Miner.* **15**, 191–195.
- Zaslavskij, A. I. & Zvincuk, R. A. (1953). *Dokl. Akad. Nauk SSSR*, **90**, 781.
- Zhang, J., Song, L., Sist, M., Tolborg, K. & Iversen, B. B. (2018). *Nat. Commun.* **9**, 4716.